830-11-15
NAS1.60:1855
JUN 2 1981

NASA Technical Paper 1855

ORIGINAL
COMPLETE

Application of a Performance Modeling Technique to an Airplane With Variable Sweep Wings

Paul C. Redin

MAY 1981

NASA

NASA Technical Paper 1855

Application of a Performance Modeling Technique to an Airplane With Variable Sweep Wings

Paul C. Redin
Dryden Flight Research Center
Edwards, California

National Aeronautics
and Space Administration

**Scientific and Technical
Information Branch**

1981

APPLICATION OF A PERFORMANCE MODELING TECHNIQUE TO AN AIRPLANE WITH VARIABLE SWEEP WINGS

Paul C. Redin
Dryden Flight Research Center

INTRODUCTION

Those involved in the planning for airplane performance flight testing try to (1) maximize the amount of useful data acquired from each test flight, (2) provide accurate information so real-time control room decisions can be made if a test flight under way must be altered, and (3) minimize flight test time in order to reduce costs. One of the tools that can help the flight planner achieve these objectives is a performance model. The performance model discussed in this paper is a computer program that calculates predicted airplane performance in terms of parameters such as time elapsed, fuel used, range traveled, rate of climb, excess thrust, rate of change of specific energy, and normal acceleration.

To calculate performance accurately for a specific airplane, the model must be adjusted and validated with actual flight test results. Reference 1 describes a concept for adjusting a performance model by correcting the error between model-predicted excess thrust and flight-measured excess thrust with separate corrections to thrust and drag. The adjusted model is then validated by comparing model-predicted performance with flight-measured performance.

Reference 1 also describes the application of this modeling concept to an F-104G airplane. In reference 2, the same modeling concept is applied to a YF-12C airplane. Both of these studies were limited to maneuvers flown at maximum afterburning power by an airplane with fixed wing geometry. The study reported in this paper extends the application of the concept to an airplane with variable wing sweep at intermediate and below intermediate power settings. For continuity between this and the previous applications, maximum afterburning operation was also modeled.

SYMBOLS AND ABBREVIATIONS

D	drag, N
F	thrust, N
F_{ex}	excess thrust, $F - D$, N
g	acceleration due to gravity, m/sec^2
$\dot{h}$	rate of climb, m/sec
K_D	modeling coefficient for drag
K_F	modeling coefficient for thrust
K_w	modeling coefficient for fuel flow rate
PLA	power lever angle, deg
SFC	specific fuel consumption, kg/sec/N
TACT	transonic aircraft technology
V	true airspeed, m/sec
$\dot{V}$	flightpath acceleration, m/sec^2
w	fuel flow rate, kg/sec

Subscripts:

m	measured
p	predicted by unadjusted model
t	calculated based on test day conditions

Superscript:

$'$	based on actual test value independent of modeling assumption

MODEL CONCEPT AND ASSUMPTIONS

The conceptual basis of the performance model discussed in this paper is developed in detail in references 1 and 2. Briefly, this concept states that the performance of an airplane can be calculated (modeled) from predicted thrust and drag characteristics suitably adjusted by modeling coefficients that are based on the difference between model predictions and flight measurements and the assumption that the predicted specific fuel consumption (SFC) is equal to actual test SFC. The implications of this assumption for the mathematical expression of the modeling concept are given in appendix A. The predicted thrust, drag, and fuel flow rate are multiplied by the appropriate coefficients and then used to calculate performance. If the modeling coefficients correlate (agree) for separate maneuvers flown under similar conditions, and measured flight-test performance can be adequately predicted (matched), the model is considered validated.

The criterion used in references 1 and 2 to consider matching to be adequate is for predicted time elapsed and fuel used to be within ±5 percent of the measured values. The same criterion is used in this study. No numerical criterion is assigned to model coefficient correlation. The important considerations for the modeling coefficients are uniformity of trends and the general agreement of coefficients generated from different types of maneuvers.

This approach to performance modeling does not provide any information about the actual values of thrust and drag. It only suggests a way to adjust the thrust and drag values based on predicted propulsion and aerodynamic characteristics so that measured performance can be matched by the model. However, if the predicted SFC does, in fact, equal actual test SFC, or their functional relationship is known mathematically, actual thrust and drag can be determined. Since actual test gas generator installed thrust was available in the data base used in this study, it was possible to calculate actual test SFC and compare it with predicted SFC. It was also possible to calculate a separate set of modeling coefficients based on actual test thrust and drag without resorting to the basic modeling assumption. In appendix B these coefficients are defined and the equations are developed that relate them to the coefficients defined in appendix A.

PERFORMANCE FLIGHT TESTS

Test Airplane

The F-111A airplane (fig. 1) is a high performance military airplane powered by two Pratt & Whitney TF30-P-3 afterburning turbofan engines. Takeoff gross weight is approximately 35,600 kilograms. The production variable sweep wing on the test airplane was replaced with a supercritical variable sweep wing as part of the transonic aircraft technology (TACT) research program, which is described in reference 3. Reference 3 also gives a detailed description of the test airplane.

Test Data

The flight data used for the development and validation of the performance model discussed in this paper were obtained from maneuvers flown during the TACT research program. The maneuvers included constant-Mach-number climbs, level accelerations and decelerations, descents, pushover pullups, and windup turns. While not specifically flown for this performance modeling study, the maneuvers were adequate for the development of the model. The performance data used in this study were not corrected for non-standard-day temperatures because a correction for temperature could be made in the propulsion model. This study used data only from those maneuvers flown at subsonic Mach numbers and at power settings of maximum afterburning, intermediate (military), and below intermediate (cruise). In addition to the flight test parameters used for performance modeling, the data base included actual test installed thrust calculated using the gas generator method described by J. J. Gritzer in In-Flight Performance Determination for TF30-P-3 Engine (Rept. PWA-3106, Pratt & Whitney Aircraft (East Hartford, Conn.), rev. 1968). Also included was the drag based on this gas generator thrust.

PERFORMANCE MODEL

Propulsion

The propulsion model consisted of tables of thrust and fuel flow rate as a function of Mach number, altitude, power setting, and temperature. These characteristics were obtained from the aircraft manufacturer (Propulsion Data Substantiation—Standard Aircraft Characteristics Charts and Regular Flight Manual, F-111A Numbers 31 Through 159, by R. F. Endres, M. A. J. Ruch, and P. C. Leamer, FZA-12-065, General Dynamics, Fort Worth Div., July 25, 1968). The tables used represent steady-state, installed-engine performance for the TF30-P-3 engine. Maximum afterburning and intermediate power settings could be selected in the model independent of measured power lever angle (PLA). The relationship between model power settings below intermediate and measured power lever angle was derived from a ground thrust run. The propulsion model did not incorporate data for partial afterburning power settings.

Aerodynamics

The aerodynamic model consisted of tables of drag coefficient and angle of attack as a function of Mach number and lift coefficient. A separate model or set of tables was included for each of the three wing sweep angles investigated: 26°, 36°, and 58°. These characteristics were obtained from reference 4 and correspond to trimmed flight at an average dynamic pressure of 28.73 kN/m^2. The aerodynamic characteristics in reference 4 were based primarily on maneuvers flown at cruise power, a power setting less than intermediate. The fact that the wing had a supercritical airfoil was of no special significance to this study. This aerodynamic model was not derived from or correlated with the propulsion model.

Trajectory Program

The propulsion and aerodynamic models described above were incorporated into a computer trajectory program which calculated all relevant performance parameters for a given flight maneuver. The trajectory program also included the modeling coefficients and a mathematical model of the earth and atmosphere. Climbs, descents, accelerations, and decelerations were described by Mach number as a function of altitude in the computer program. Pushover-pullup and windup-turn maneuvers were described by lift coefficient and bank angle as a function of time.

MODEL DEVELOPMENT AND VALIDATION

Maximum Power Operation

The model was developed first for maximum afterburning power based on subsonic level accelerations and constant-Mach-number climbs. During a constant-Mach-number climb actual Mach number sometimes varied by as much as 0.1. The climbs were flown at target Mach numbers from 0.7 to 0.9. The altitude for the level accelerations typically varied less than 300 meters during a maneuver. The level accelerations were flown at target altitudes from 3000 meters to 9400 meters.

The first step in correlating the modeling coefficients was to collect the coefficients for maneuvers flown at the same wing sweep angle. Figure 2 illustrates this step by showing the values for the modeling coefficients K_D and K_F as a function of altitude for 26° of wing sweep. Since by definition K_F equals K_w (app. A, eq. (15)), K_w is not shown. A thrust or drag coefficient value of 1.0 means that the predicted values equal the test values. A value less than 1.0 means that the test value is lower than predicted, and a value greater than 1.0 means that the test value is higher than predicted. The coefficients for the two types of maneuvers agree fairly well. There was no identifiable trend with Mach number. Both K_D and K_F varied with altitude.

Figures similar to figure 2 were constructed for 36° and 58° of wing sweep. The values of the coefficients for each wing sweep angle were then faired with one line. These faired values are shown in figure 3. The values for K_D show some variation with wing sweep angle (less than that between maneuvers for any single wing sweep angle, however); the values for K_F form essentially one line. The values in figure 3 were faired again so that K_D and K_F were each represented by one line. These final faired values were applied as modeling coefficients to the predicted model characteristics for each of the three wing sweep angles.

Figures 4(a), 4(b), and 4(c), for wing sweep angles of 26°, 36°, and 58°, respectively, show the values of time elapsed and fuel used as measured in flight compared with values predicted by the model for maximum afterburning subsonic constant-Mach-number climbs. This comparison is called a performance match. The

symbols show the model predictions with and without coefficients. The model with coefficients means that K_D and K_F are equal to the values shown in figure 3. The model without coefficients means that K_D and K_F are equal to a constant value of 1.0. The latter values indicate the performance predicted by the unadjusted model. The performance match for both cases is good. The change in predicted performance due to the application of the modeling coefficients is small in spite of the fact that the modeling coefficient K_D indicates a 40 percent adjustment to the predicted drag at altitudes from 3600 to 8000 meters (fig. 3). Because excess thrust is high at these altitudes, the large percentage adjustment to drag has a small effect on the agreement between predicted and flight performance.

To understand why a 40 percent adjustment to drag is needed, it is helpful to compare the modeling coefficients just presented, K_D and K_F, with another set, K_D' and K_F', based on actual test thrust and drag from the gas generator method. Figure 5 shows these four coefficients as a function of altitude for a constant-Mach-number climb at maximum afterburning power and 26° of wing sweep, the same maneuver as shown in figure 4(a). Also shown is the percentage of error in SFC calculated from equation (31) (app. B). Figure 5 illustrates the relationships defined by equations (30) and (32). At 10,350 meters, the error in SFC is zero, and K_F' equals K_F. Since K_F equals K_w (eq. (14)), K_F' also equals K_w. In addition, K_D' equals K_D at this point. However, when the SFC error is not equal to zero, the modeling coefficients are not equal. Their relative differences are defined by equation (25). When predicted thrust, F_p, is greater than predicted drag, D_p, $K_D' - K_D$ will be greater than $K_F' - K_F$. At 4000 meters, for example, $K_D' - K_D = 0.3$, while $K_F' - K_F = 0.1$. We can conclude that since K_D is a function of SFC_p (eq. (17)), any error in SFC_p is magnified as it is reflected in K_D. This effect and the fact that the drag model was not correlated with the thrust model are the basic reasons for the 40 percent adjustment to drag noted above. Therefore, K_D cannot be relied upon to give an accurate indication of drag error. It remains to be said that when the SFC error is zero (SFC_p equals SFC_t), the thrust and drag calculated from the basic modeling assumption are equal to the actual test thrust and drag.

To illustrate that a good performance match could be obtained with coefficients based on actual test thrust and drag, the modeling coefficients K_D' and K_F' were faired and correlated for the same maneuvers and in the same manner as K_D and K_F in figures 2 and 3. These coefficients, together with K_w, were then used in the model to calculate a performance match similar to figure 4(a). The results are shown in figure 6 and are essentially the same as the match shown in figure 4(a), even though the error in SFC was in the vicinity of 10 percent over much of the maneuver.

Intermediate Power Operation

Performance match.—The results of correlating the modeling coefficients for intermediate power are shown in figure 7. These values were obtained by a fairing procedure similar to that described above for figures 2 and 3. For 26° and 58° of wing sweep, the values for K_D were the same. This was also true for K_F. Neither modeling coefficient showed any significant trend with Mach number or altitude. For use in the model the values for K_F were faired as one line for all wing sweep angles. The values used in the model for K_D were those shown in figure 7. The resulting performance match is shown in figure 8. The performance match for the model with coefficients is good, while that for the model without coefficients is poor. Because excess thrust is low for these maneuvers, small coefficient adjustments to predicted thrust and drag have a large effect on predicted performance.

Comparison with maximum power.—A comparison of figures 7 and 3 indicates that the values for the modeling coefficients K_D and K_F at intermediate power are significantly different from those at maximum afterburning power for the same type of maneuver and Mach number/altitude conditions. This difference bears explanation. The values of F_p, w_p, and SFC_p in the propulsion model are obviously different for the intermediate and maximum afterburning power settings. Since the flight values of w_m and F_{ex_m} also change with power setting, the value of K_F may or may not change. The fact that K_F is different merely reflects the difference in the adjustment the intermediate power setting model requires compared with the adjustment the maximum afterburning model requires to match flight data. Nothing in the modeling concept requires that the value of K_F be the same for all power settings.

The reason for the change in K_D is not so obvious, since the same aerodynamic model was used for all power settings. To help explain the change in K_D, figure 9 presents the four modeling coefficients, K_D, K_D', K_F, K_F', and SFC error as a function of altitude for a subsonic constant-Mach-number climb at intermediate power and 26° of wing sweep (the same maneuver as shown in fig. 8(a)). In figure 9 the SFC error ranges from 3 to 4 percent, compared with a range from -8 to 12 percent for the maximum afterburning power maneuver in figure 5. As can be seen from a comparison of the difference between K_D and K_D' and K_F and K_F' in figures 9 and 5, the larger the magnitude of the SFC error the larger the difference between the coefficients. Equations (30) and (32) define this relationship. Since the SFC error for maximum afterburning power is larger for the most part than for intermediate power, the difference between the coefficients is larger. Thus, the change in K_D illustrates that different adjustments to predicted drag may be required for different power settings even when the same aerodynamic model is used and when the predicted drag is close to the actual test values.

Another point worthy of note is that the values of K_D' in figure 9 differ from those in figure 5. The difference probably appears because the aerodynamic model was

based primarily on a fairing of maneuvers flown at cruise power settings (less than intermediate), and because the model as used did not incorporate provision for variable dynamic pressure. Reference 4 points out and illustrates that this aerodynamic model can differ from the flight test data for intermediate and maximum afterburning power settings even when the effects of variable dynamic pressure are incorporated.

Operation Below Intermediate Power

Modeling coefficients were calculated at several power settings below intermediate for descent and level deceleration maneuvers at the three wing sweep angles. Figure 10(a) shows values of K_D and K_F as a function of Mach number for 18 level decelerations at several altitudes. These values were calculated with power lever angles in the model equal to those measured. The values of K_D have approximately the same variation as those for maximum afterburning power. The values of K_F show far greater variation than those for either maximum afterburning or intermediate power. However, since each different PLA represents an essentially different model, the coefficient values might be expected to change with PLA (as discussed in the previous section). Figure 10(b) shows the values of K_D and K_F as a function of PLA for the level decelerations through a Mach number of 0.8. The value of K_D stays reasonably constant as PLA increases. There is no correlation between K_F and PLA. Other data show that even at the same altitude and PLA, the values of K_F for different maneuvers and flights do not agree. This could be the result of several factors. For one thing, the model was sensitive to uncertainties in the measured values of PLA. A change in PLA of 2° at low power settings could cause a change of 0.1 in K_F. For another, the relationship between PLA and the propulsion model power setting was established in an engine ground run. This relationship would not necessarily be representative of conditions at altitude. These considerations indicate that for the propulsion model used in this study, PLA was not an adequate representation of power setting. The model was therefore not considered to be validated at power settings below intermediate.

Data for engine rotor speed and engine pressure ratio were not readily available and thus could not be used to indicate power setting. Fuel flow rate could be used as a power setting indicator. However, this would require both K_F and K_w to equal 1.0 and all corrections to be lumped into K_D. This approach voids the basic modeling concept of this study and was not considered further.

Dynamic Maneuvers

In references 1 and 2 the validation of the performance modeling concept was limited to climbing and accelerating maneuvers flown at a normal load factor of 1.0. This section describes an attempt to apply the concept to two types of dynamic maneuvers—pushover pullups and windup turns. These maneuvers are characterized

by large, rapid variations in angle of attack, lift coefficient, and normal load factor. For performance calculations, dynamic maneuvers were specified in the model by values of lift coefficient and bank angle as a function of time.

Figure 11 shows K_D and K_F as a function of lift coefficient for the pullup portion of a typical pushover-pullup maneuver and for a windup-turn maneuver, both flown at a power setting less than intermediate. The value of K_D increases over the range of lift coefficients shown, while the value of K_F does not change. The values for both maneuvers are essentially the same.

An attempt was made to correlate the modeling coefficients for several pushover-pullup and windup-turn maneuvers performed over a range of Mach numbers, altitudes, power settings (all of which were below intermediate, however), and wing sweep angles. There was no correlation with PLA. This is the same result as discussed above for descents and level decelerations and can be attributed to the same causes. Since no correlated values for the modeling coefficients derived from dynamic maneuvers could be achieved, the only way to demonstrate a performance match was to use coefficient values unique to each maneuver. This was done for the two maneuvers shown in figure 11.

A performance-matching criterion defined in terms of time elapsed and fuel used is not realistic for dynamic maneuvers, since the amount of fuel used is insignificant (less than 13 kg for the maneuvers in fig. 11) and the time elapsed is an independent variable. A more appropriate criterion would be how well the model reconstructs excess thrust over the range of load factors flown. The other parameter chosen for matching was dive angle—the inclination of the flightpath below the horizon. Dive angle characterizes the flightpath better than Mach number and altitude, since the latter parameters change only a small amount during a dynamic maneuver.

Figure 12 shows how the model-predicted values of excess thrust and dive angle with and without coefficients compare with flight-measured values for the pushover-pullup and windup-turn maneuvers. The coefficients have a small effect on the excess thrust values. At the beginning of the maneuvers thrust and drag are relatively small, so the 20 percent adjustments shown in figure 11 for low lift coefficients have a small effect. At the end of the maneuvers, drag is very large compared to thrust. However, at these high lift coefficients K_D is approximately 1, and the 20 percent correction to thrust is not significant. Small, abrupt changes in excess thrust are hard to match either with or without modeling coefficients. The coefficients have little effect on the dive angle values for either maneuver. This is related to the small effect of the coefficients on excess thrust and the short duration of the maneuvers. The overall performance match for the two dynamic maneuvers shown was very good.

CONCLUDING REMARKS

A modeling concept previously applied to an F-104G and a YF-12C airplane was modified and applied to an F-111A airplane with a supercritical wing. The application was new in that test maneuvers were flown at different wing sweep angles and at power settings of intermediate and below. Maximum afterburning power maneuvers were also included to insure continuity between this effort and previous applications. For maximum afterburning climbs and level accelerations at three wing sweep angles, the model predicted performance in terms of time elapsed and fuel used within validation boundaries of ±5 percent. The results for intermediate power maneuvers were also within the ±5 percent limits.

A comparison between predicted and test values for specific fuel consumption (SFC) showed that since the modeling coefficient for drag, K_D, is a function of predicted SFC, large differences in SFC could cause large adjustments to drag even when predicted drag is close to actual test drag.

The modeling coefficients calculated for descents and decelerations at power settings below intermediate did not correlate, and the modeling concept was not validated for these power settings because the method used to correlate model and in-flight power settings was not adequate.

A good performance match was achieved for two dynamic maneuvers—a pushover pullup and a windup turn—using modeling coefficients unique to each maneuver.

Dryden Flight Research Center
National Aeronautics and Space Administration
Edwards, California 93523
November 21, 1980

APPENDIX A—MATHEMATICAL IMPLICATIONS OF THE PERFORMANCE MODELING CONCEPT

The basic calculation incorporated in the model can be expressed by the equations

$$(\dot{h} + \dot{V}V/g)_t = K_F F_p - K_D D_p \tag{1}$$

and

$$w_t = K_w w_p \tag{2}$$

where test day performance, represented by $(\dot{h} + \dot{V}V/g)_t$, is a function of predicted thrust and drag, F_p and D_p, multiplied by the flight-derived modeling coefficients, K_F and K_D, respectively. The third modeling coefficient, K_w, is used to adjust predicted fuel flow rate.

The values for K_F, K_D, and K_w are found by measuring flight-test conditions and solving the following equations:

$$K_F = F_t/F_p \tag{3}$$

$$K_D = D_t/D_p \tag{4}$$

$$K_w = w_m/w_p \tag{5}$$

where

$$F_t - D_t = F_{ex_m} \tag{6}$$

In order to avoid the inconvenient and difficult measurement of in-flight thrust and drag (described in ref. 5, for example), F_t and D_t are calculated on the assumption suggested in reference 1 that

$$SFC_t = SFC_p \tag{7}$$

The value of F_t is calculated from measured fuel flow rate as follows. By definition,

$$SFC_t = w_m/F_t \tag{8}$$

and

$$SFC_p = w_p/F_p \tag{9}$$

From equation (7),

$$w_m/F_t = w_p/F_p \tag{10}$$

Rearranging terms gives

$$F_t = (w_m/w_p)F_p \tag{11}$$

which can be written

$$F_t = w_m/\mathrm{SFC}_p \tag{12}$$

from equation (9), or

$$F_t = K_w F_p \tag{13}$$

from equation (5). It is then easy to calculate D_t by rearranging equation (6) as follows:

$$D_t = F_t - F_{ex_m} \tag{14}$$

A comparison of equation (13) with equation (3) shows that the basic modeling assumption requires by definition that

$$K_F = K_w \tag{15}$$

An important implication of calculating F_t in this way is that K_D is a function of SFC_p. If substitutes from equations (4) and (12) are entered for D_t and F_t, respectively, in equation (14),

$$K_D D_p = w_m/\mathrm{SFC}_p - F_{ex_m} \tag{16}$$

or

$$K_D = \frac{w_m}{\mathrm{SFC}_p D_p} - \frac{F_{ex_m}}{D_p} \tag{17}$$

Therefore, K_D is influenced by the characteristics of the propulsion model as well as the values for w_m, F_{ex_m}, and D_p.

APPENDIX B—DEVELOPMENT OF MODELING COEFFICIENTS BASED ON ACTUAL TEST THRUST AND DRAG

The modeling coefficients based on actual test thrust and drag (which are identified by primes) are defined as follows:

$$K_F' = F_t'/F_p \tag{18}$$

$$K_D' = D_t'/D_p \tag{19}$$

where F_t' and D_t' are actual test values based on measured flight conditions such that

$$F_t' - D_t' = F_{ex_m} \tag{20}$$

The actual test SFC is defined as

$$SFC_t' = w_m/F_t' \tag{21}$$

The fuel flow rate modeling coefficient K_w is the same as that defined in equation (5) in appendix A. However, K_F' is not required to be equal to K_w, since K_F' is calculated independent of the modeling assumption that SFC_t equals SFC_p. The values of K_F' and K_w may be equal, though, and in fact are whenever SFC_t' equals SFC_p.

The two sets of modeling coefficients can be related as follows. If equation (6) is combined with equation (20),

$$F_t' - D_t' = F_t - D_t \tag{22}$$

If both sides are divided by F_pD_p and the equation is rearranged,

$$F_t'/F_pD_p - F_t/F_pD_p = D_t'/F_pD_p - D_t/F_pD_p \tag{23}$$

From the modeling coefficient definitions (eqs. (3), (4), (18), and (19)),

$$K_F'/D_p - K_F/D_p = K_D'/F_p - K_D/F_p \tag{24}$$

or

$$K_D' - K_D = \frac{F_p}{D_p}(K_F' - K_F) \tag{25}$$

The expression $K_F' - K_F$ can be expanded as follows:

$$K_F' - K_F = F_t'/F_p - F_t/F_p \tag{26}$$

From the definitions in equations (21) and (8),

$$K_F' - K_F = \frac{w_m}{F_p SFC_t'} - \frac{w_m}{F_p SFC_t} \tag{27}$$

Converting to a common denominator gives

$$K_F' - K_F = \frac{w_m}{F_p} \frac{SFC_t - SFC_t'}{SFC_t' SFC_t} \tag{28}$$

From equation (7),

$$K_F' - K_F = \frac{w_m}{SFC_p F_p} \frac{SFC_p - SFC_t'}{SFC_t'} \tag{29}$$

and finally, from equations (9) and (5),

$$K_F' - K_F = K_w \Delta SFC \tag{30}$$

where

$$\Delta SFC = \frac{SFC_p - SFC_t'}{SFC_t'} \tag{31}$$

Equation (25) can then be written

$$K_D' - K_D = \frac{F_p}{D_p} K_w \Delta SFC \tag{32}$$

Equations (30) and (32) illustrate how the difference in the modeling coefficients is proportional to the difference in the values of SFC, the fuel flow rate modeling coefficient K_w, and, for drag, the ratio of predicted thrust to predicted drag.

REFERENCES

1. Marshall, Robert J.; and Schweikhard, William G.: Modeling of Airplane Performance From Flight-Test Results and Validation With an F-104G Airplane. NASA TN D-7137, 1973.

2. Redin, Paul C.: A Performance Model of the YF-12C Airplane. YF-12 Experiments Symposium, NASA CP-2054, Vol. 3, 1978, pp. 509-534.

3. Painter, Weneth D.; and Caw, Lawrence J.: Design and Physical Characteristics of the Transonic Aircraft Technology (TACT) Research Aircraft. NASA TM-56048, 1979.

4. Cooper, James M., Jr.; Hughes, Donald L.; and Rawlings, Kenneth III: Transonic Aircraft Technology - Flight-Derived Lift and Drag Characteristics. Vols. I and II. AFFTC-TR-77-12, July 1977.

5. Arnaiz, Henry H.: Techniques for Determining Propulsion System Forces for Accurate High Speed Vehicle Drag Measurements in Flight. AIAA Paper 75-964, Aug. 1975.

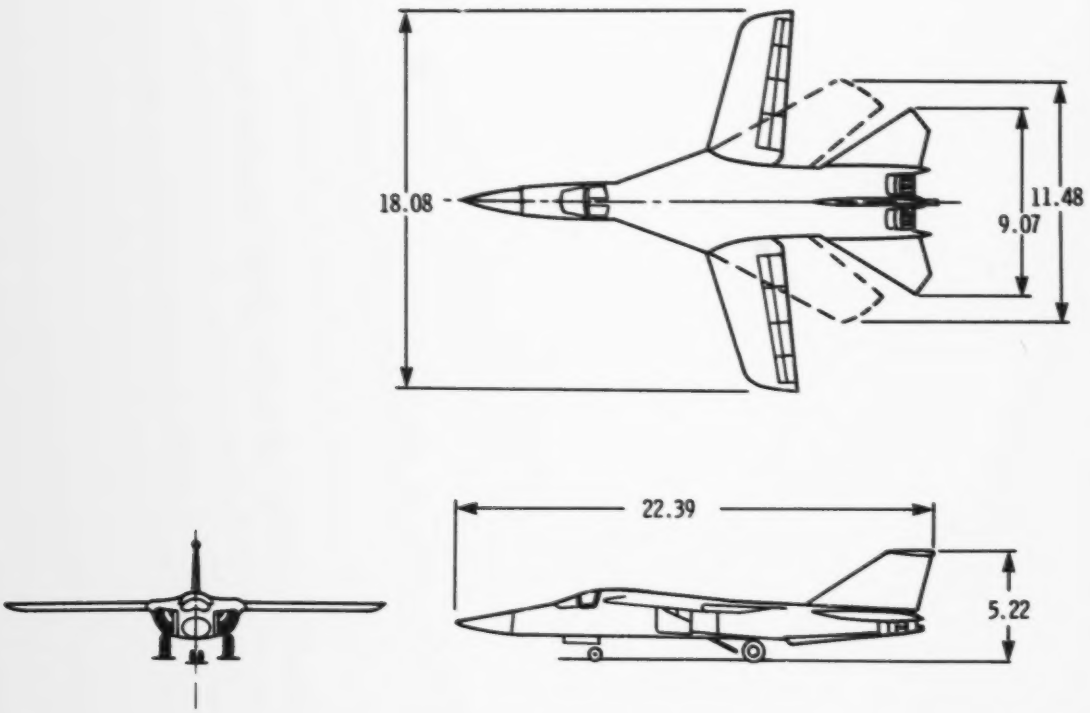

Figure 1. Three-view drawing of F-111A TACT aircraft. Dimensions are in meters.

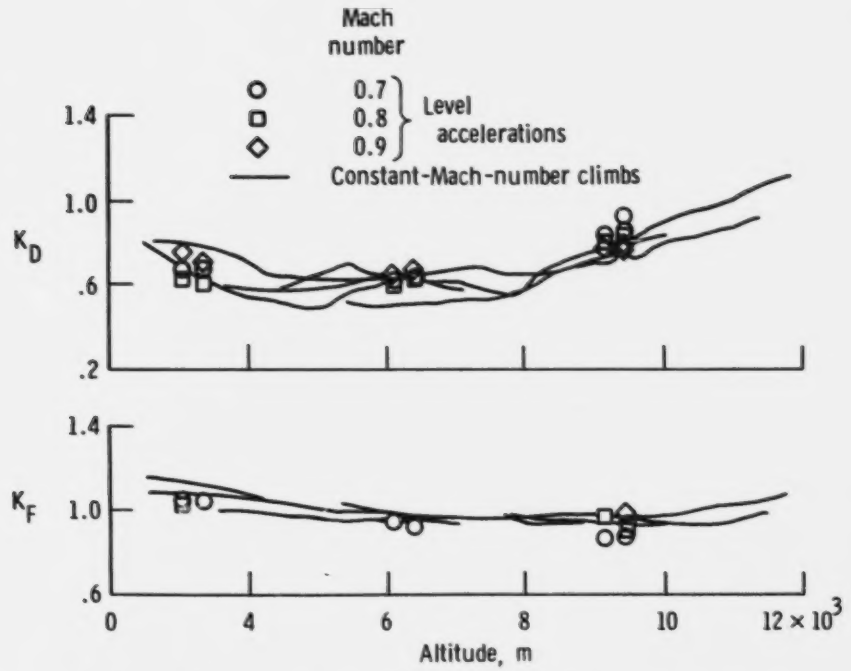

Figure 2. Modeling coefficients for subsonic constant-Mach-number climbs and level accelerations. 26° wing sweep angle, maximum afterburning power.

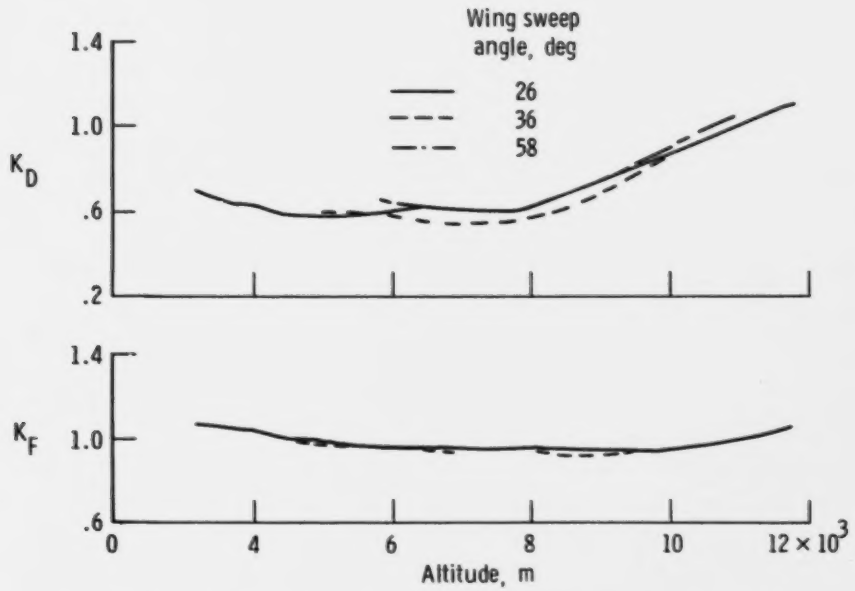

Figure 3. Modeling coefficient correlation for subsonic constant-Mach-number climbs and level accelerations. Maximum afterburning power.

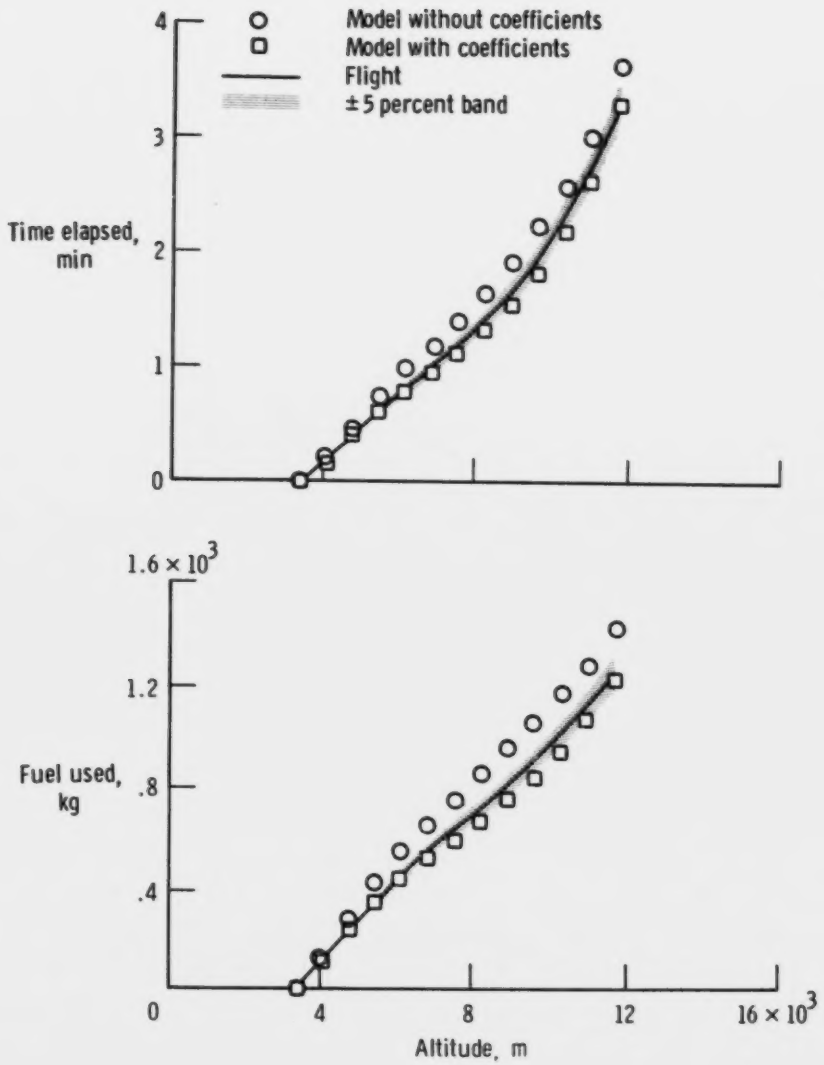

(a) 26° wing sweep angle.

Figure 4. Comparison of model predictions with flight-measured values for typical constant-Mach-number climbs at maximum afterburning power.

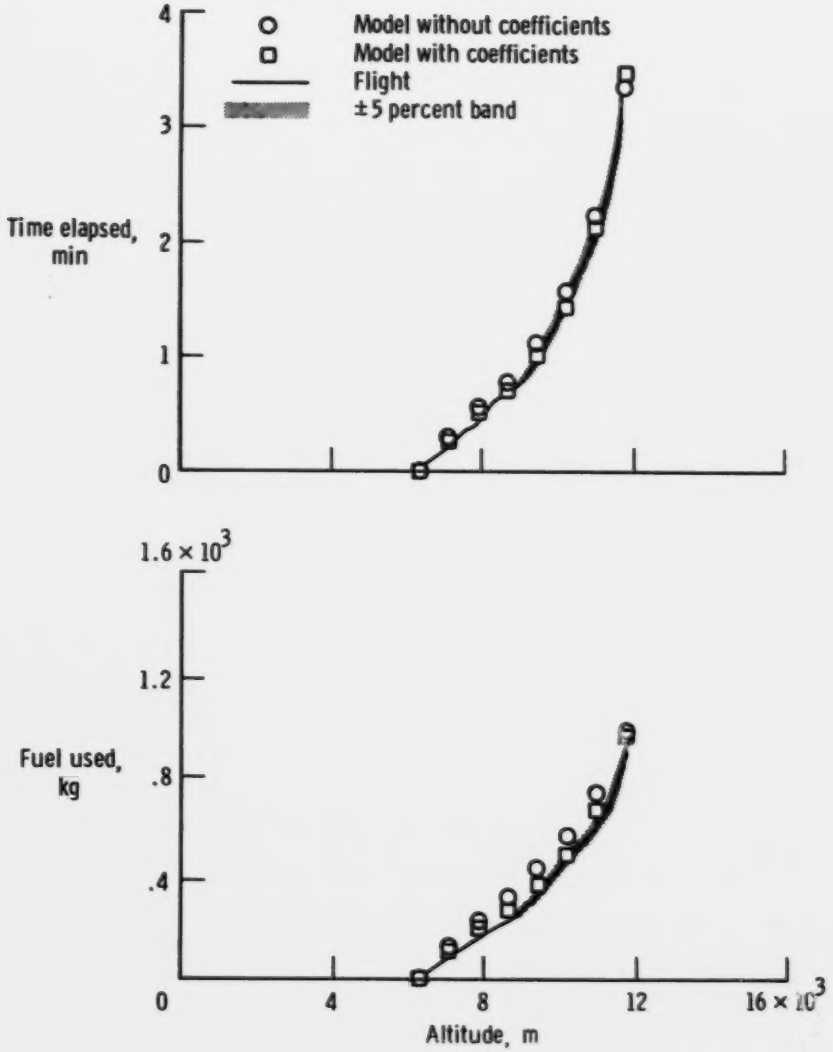

(b) 36° wing sweep angle.

Figure 4. Continued.

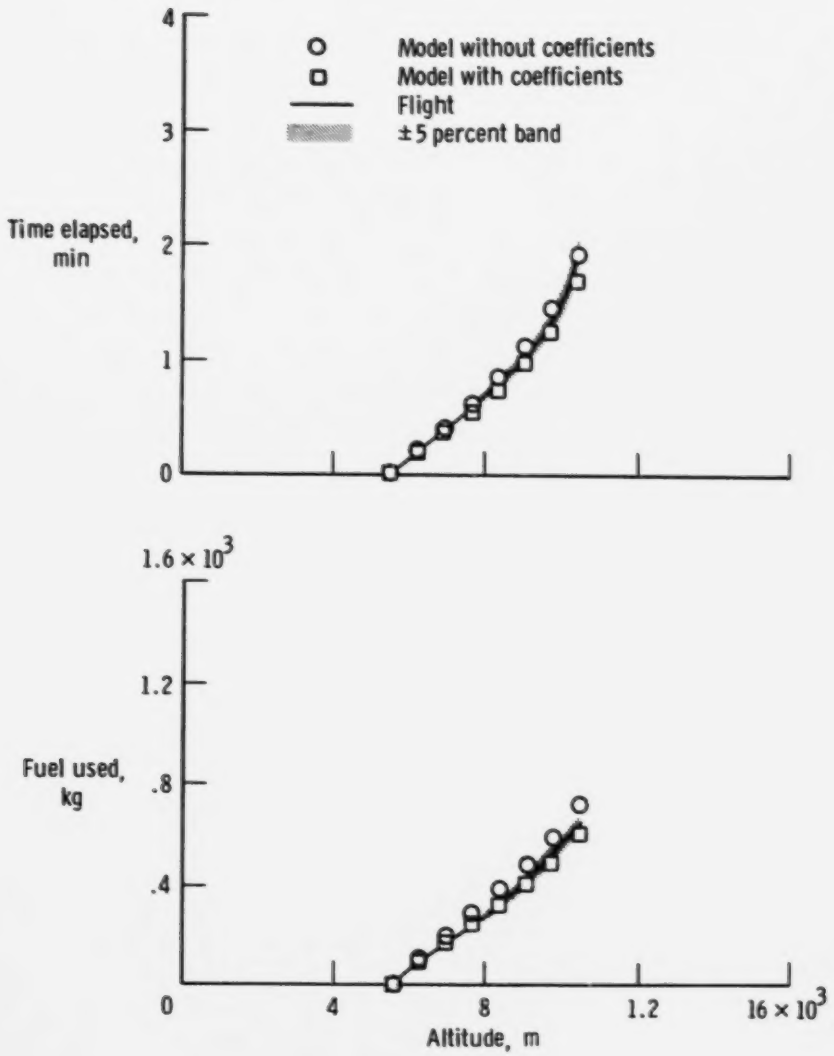

(c) 58° wing sweep angle.

Figure 4. Concluded.

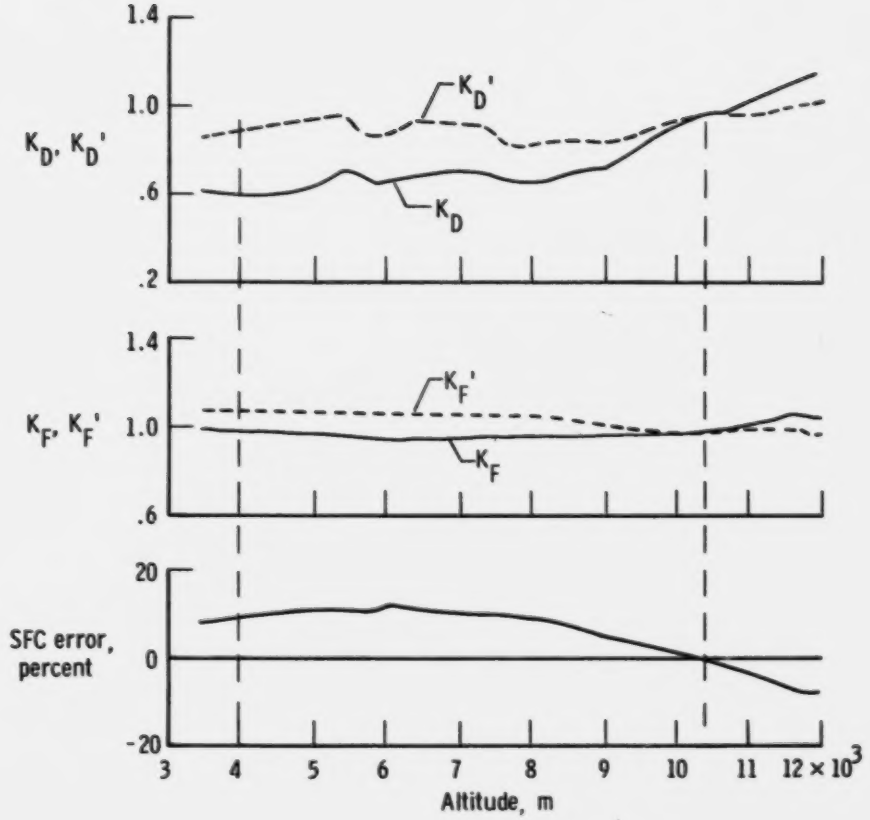

Figure 5. Modeling coefficients and SFC error for a typical subsonic constant-Mach-number climb. 26° wing sweep angle, maximum afterburning power.

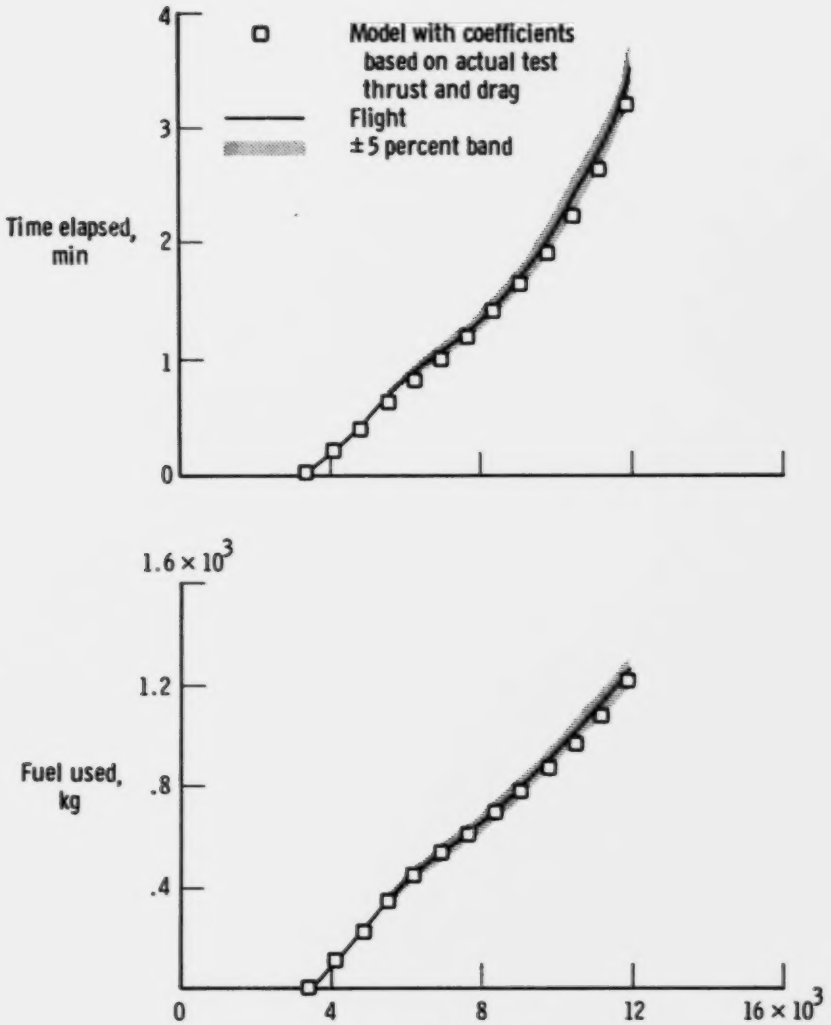

Figure 6. Comparison of model predictions with flight-measured values using modeling coefficients based on actual test thrust and drag. Same maneuver as in figure 4(a).

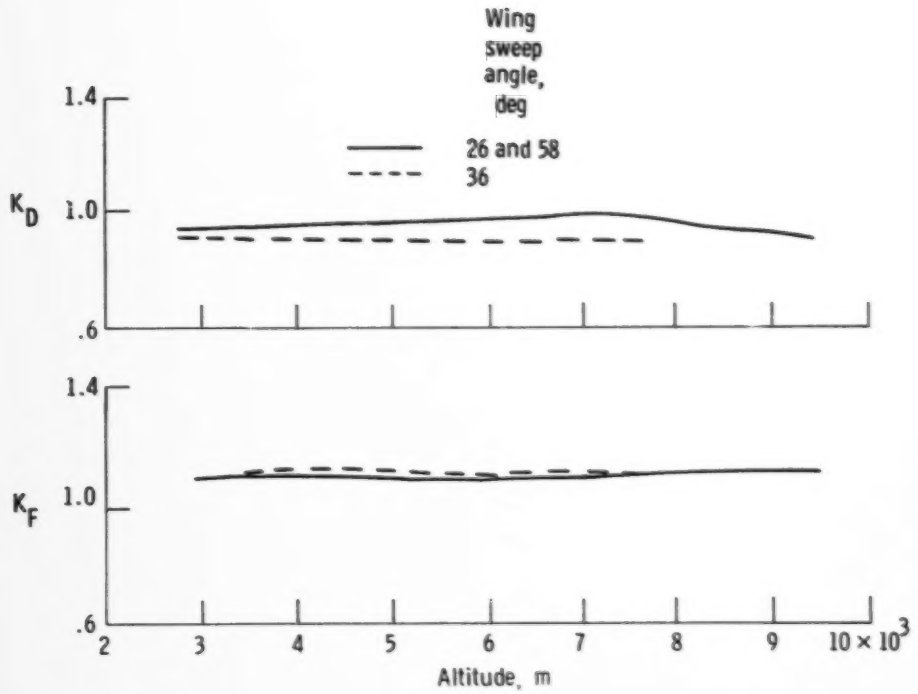

Figure 7. Modeling coefficient correlation for subsonic constant-Mach-number climbs and level accelerations. Intermediate power.

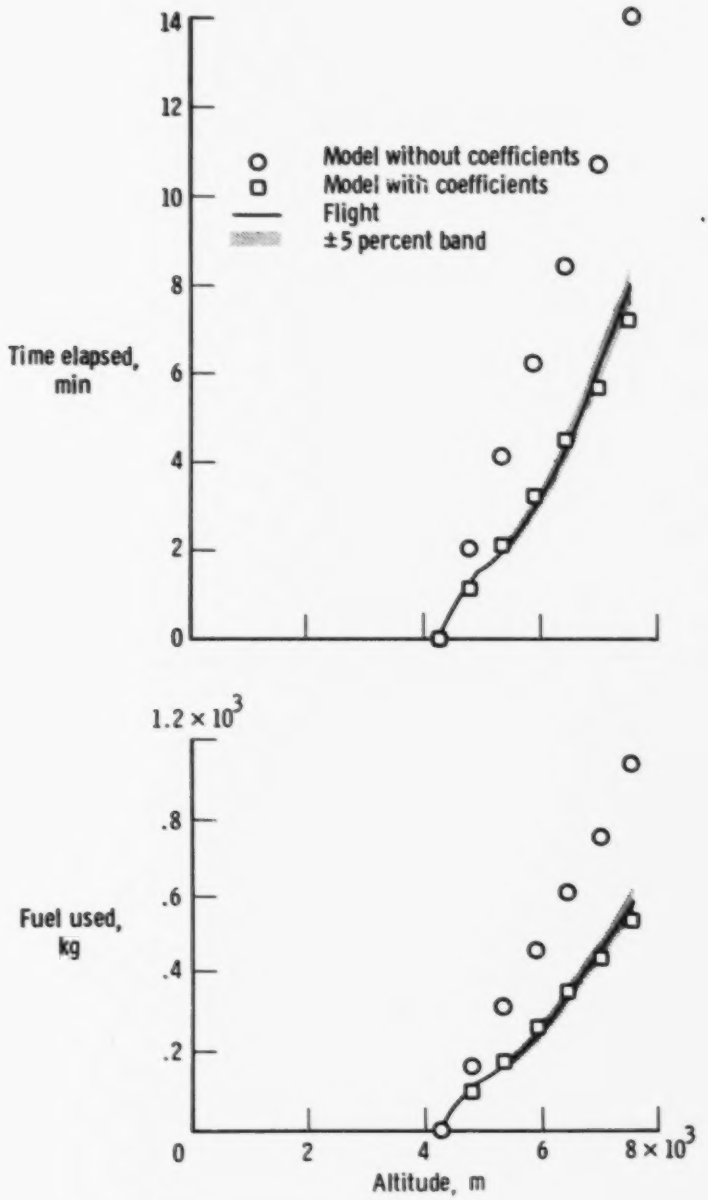

(a) 26° wing sweep angle.

Figure 8. Comparison of model predictions with flight-measured values for typical constant-Mach-number climbs at intermediate power.

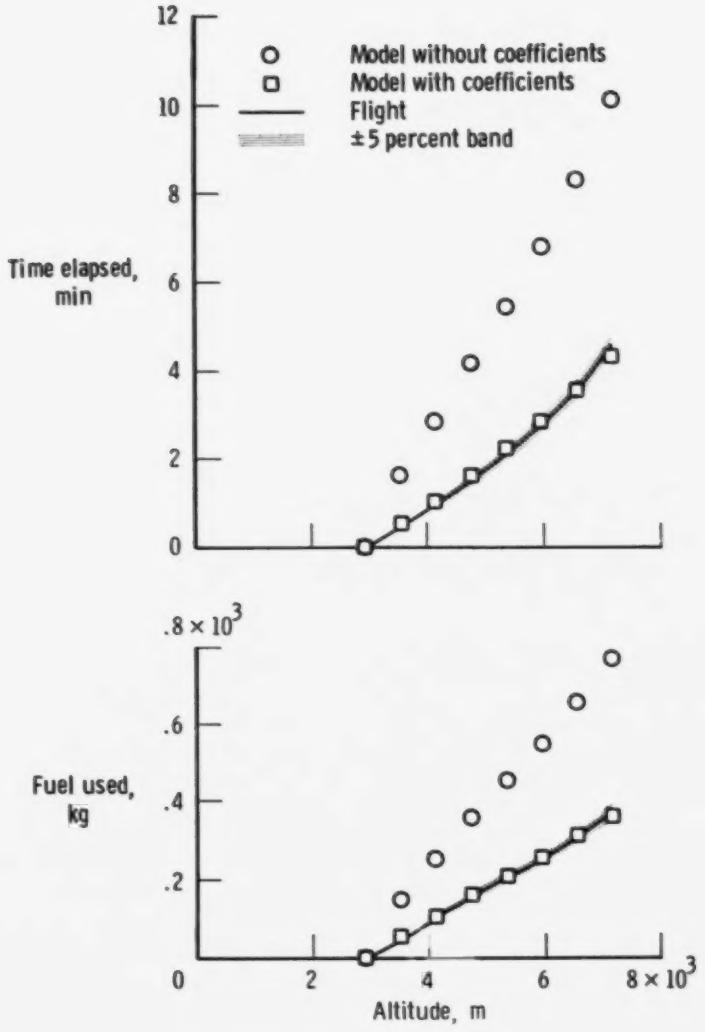

(b) 36° wing sweep angle.

Figure 8. Continued.

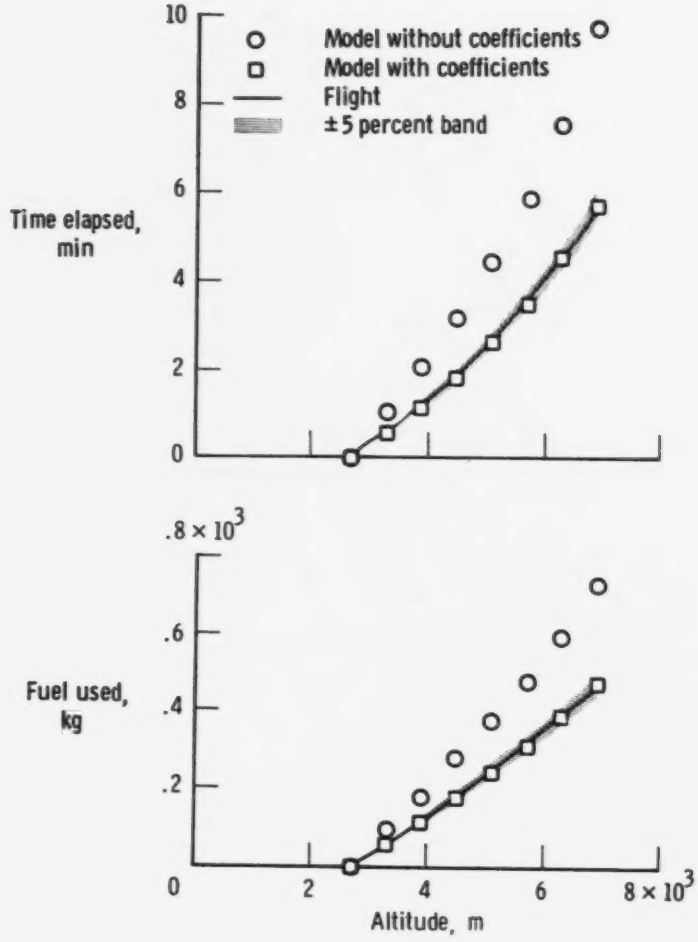

(c) 58° wing sweep angle.

Figure 8. Concluded.

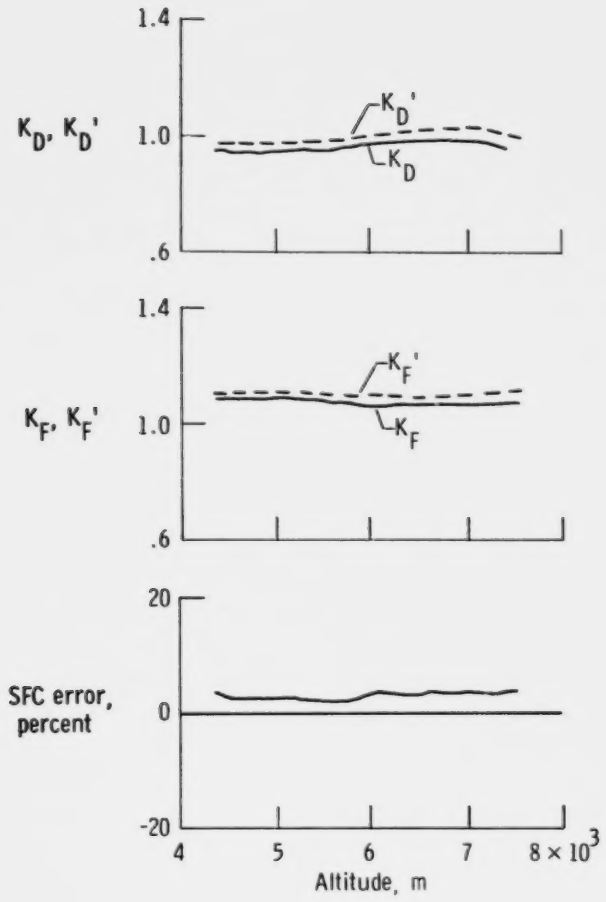

Figure 9. Modeling coefficients and SFC error for a typical subsonic constant-Mach-number climb. 26° wing sweep angle, intermediate power.

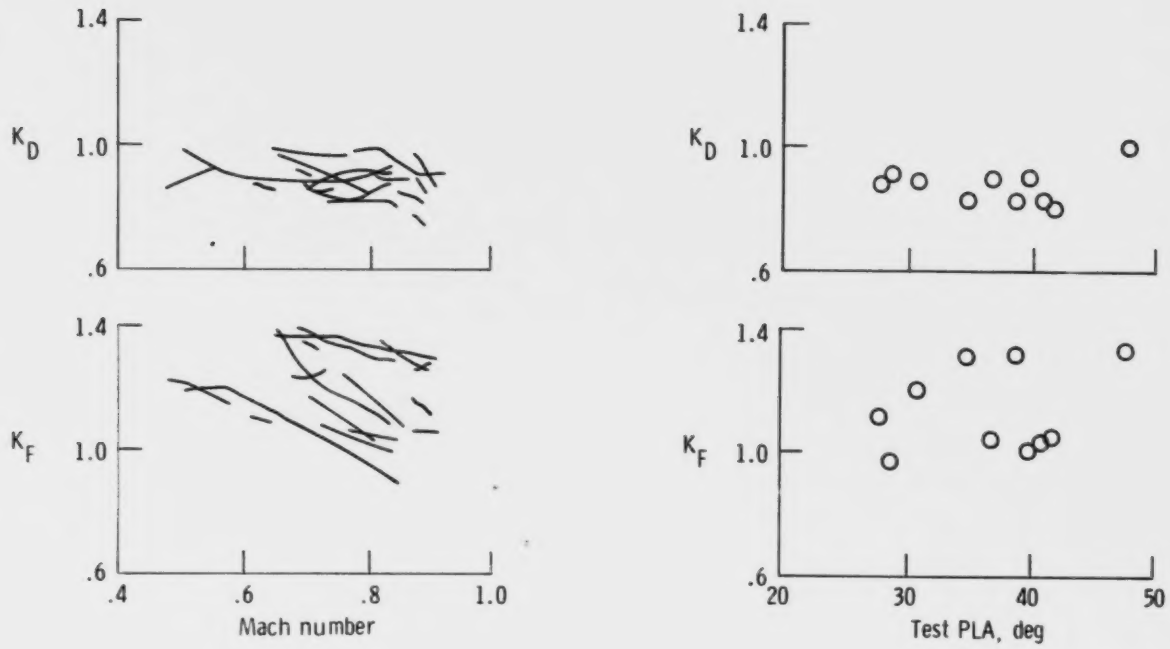

(a) All decelerations. *(b) Decelerations through Mach 0.8.*

Figure 10. Modeling coefficients for level decelerations at power settings below intermediate. All wing sweep angles.

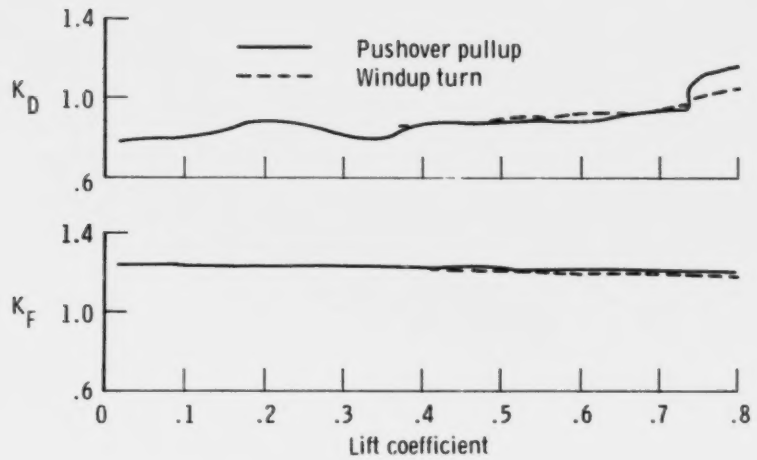

Figure 11. Modeling coefficients for a typical pushover pullup and windup turn. 36° wing sweep angle.

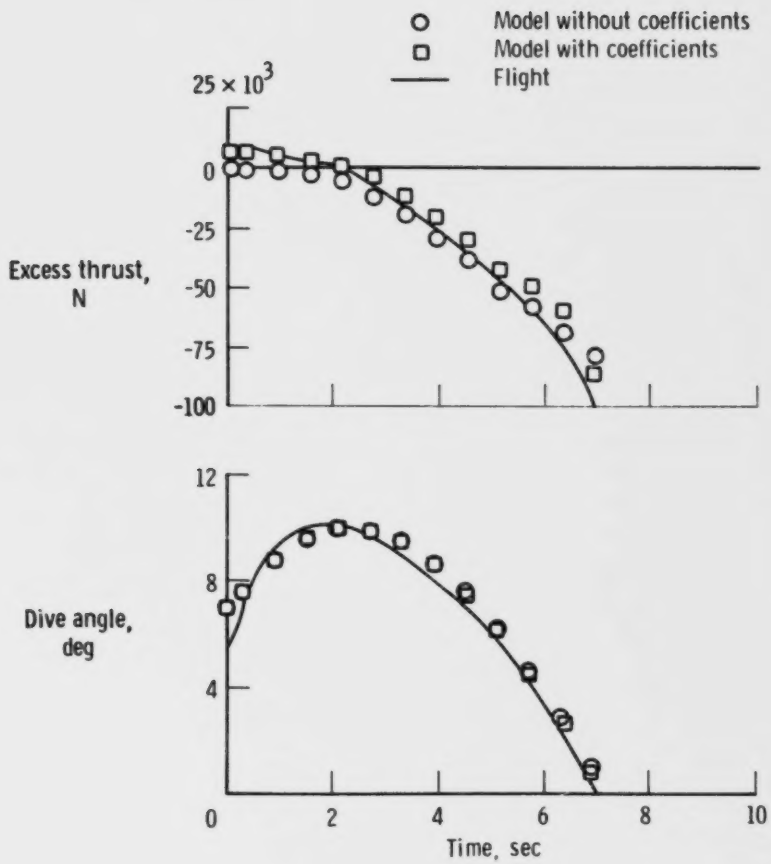

(a) Pushover pullup.

Figure 12. Comparison of model predictions with flight-measured values for pushover-pullup and windup-turn maneuvers.

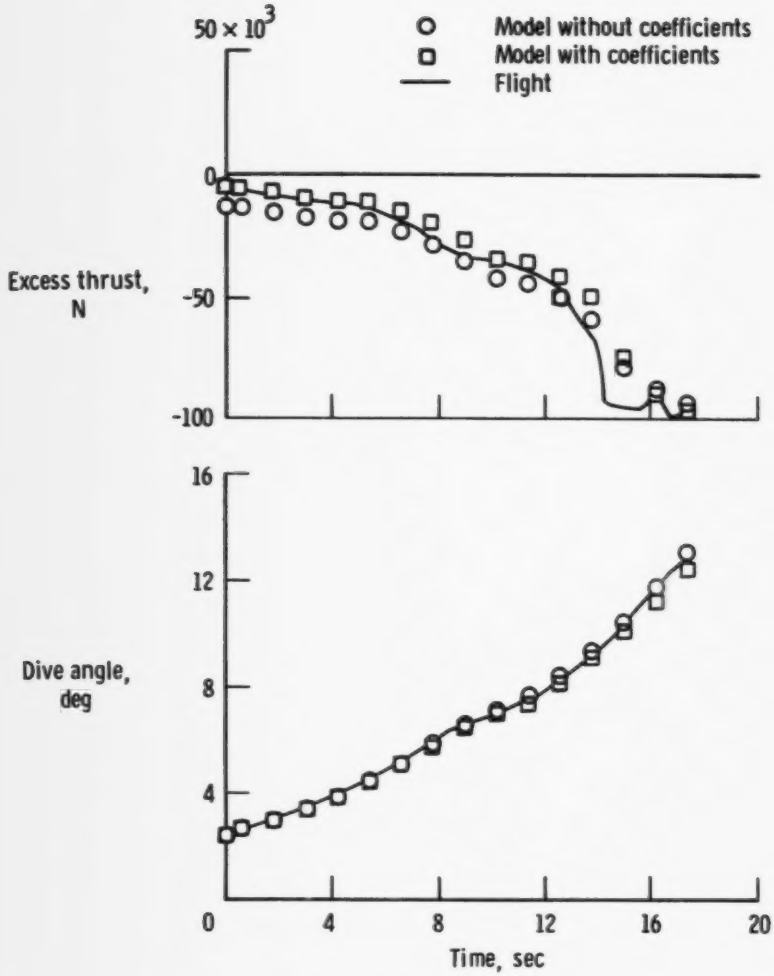

(b) Windup turn.

Figure 12. Concluded.

1. Report No.	2. Government Accession No.	3. Recipient's Catalog No.
NASA TP-1855		

4. Title and Subtitle	5. Report Date
APPLICATION OF A PERFORMANCE MODELING TECHNIQUE TO AN AIRPLANE WITH VARIABLE SWEEP WINGS	May 1981
	6. Performing Organization Code: RTOP 505-43-24

7. Author(s)	8. Performing Organization Report No.
Paul C. Redin	H-1131
	10. Work Unit No.

9. Performing Organization Name and Address	11. Contract or Grant No.
NASA Dryden Flight Research Center P.O. Box 273 Edwards, California 93523	
	13. Type of Report and Period Covered: Technical Paper

12. Sponsoring Agency Name and Address	14. Sponsoring Agency Code
National Aeronautics and Space Administration Washington, D.C. 20546	

15. Supplementary Notes

16. Abstract

A performance modeling concept previously applied to an F-104G and a YF-12C airplane was applied to an F-111A airplane. This application extended the concept to an airplane with variable sweep wings. The performance model adequately matched flight test data for maneuvers flown at different wing sweep angles at maximum afterburning and intermediate power settings. For maneuvers flown at less than intermediate power, including dynamic maneuvers, the performance model was not validated because the method used to correlate model and in-flight power setting was not adequate. Individual dynamic maneuvers were matched successfully by using adjustments unique to each maneuver.

17. Key Words (Suggested by Author(s))	18. Distribution Statement
Computer modeling TACT F-111A airplane Performance	Unclassified—Unlimited STAR category 05

19. Security Classif. (of this report)	20. Security Classif. (of this page)	21. No. of Pages	22. Price*
Unclassified	Unclassified	33	A03

For sale by the National Technical Information Service, Springfield, Virginia 22161

NASA-Langley, 1981

National Aeronautics and Space Administration

Washington, D.C.
20546

Official Business
Penalty for Private Use, $300

SPECIAL FOURTH CLASS MAIL
BOOK

Postage and Fees Paid
National Aeronautics and
Space Administration
NASA-451

2 1 1U,D, 080781 S02378DU
GOVERNMENT PRINTING OFFICE
ATTN: MAE S COLLINS, CHIEF LIBRARY DIV
5236 EISENHOWER AVE
ALEXANDRIA VA 22304

NASA

POSTMASTER: If Undeliverable (Section 158 Postal Manual) Do Not Return